Blocking Angiopoietin-2 Promotes Vascular Damage and Growth Inhibition in Mouse Tumors Treated with Small Doses of Radiation

Pauliina Kallio[1,2], Elina Jokinen[1], Jenny Högström[1], Suvendu Das[1], Sarika Heino[1,2], Marianne Lähde[1,2], Jefim Brodkin[1,2], Emilia A. Korhonen[1,3], and Kari Alitalo[1,2,3]

ABSTRACT

Abnormal vasculature in tumors leads to poor tissue perfusion and cytostatic drug delivery. Although drugs inducing vascular normalization, for example, angiopoietin-2 (Ang2)-blocking antibodies, have shown promising results in preclinical tumor models, clinical studies have so far shown only little efficacy. Because Ang2 is known to play a protective role in stressed endothelial cells, we tested here whether Ang2 blocking could enhance radiation-induced tumor vascular damage. Tumor-bearing mice were treated with anti-Ang2 antibodies every 3 or 4 days starting 3 days before 3 × 2 Gy or 4 × 0.5 Gy whole-body or tumor-focused radiation. Combination treatment with anti-Ang2 and radiation improved tumor growth inhibition and extended the survival of mice with melanoma or colorectal tumors. Single-cell RNA-sequencing revealed that Ang2 blocking rescued radiation-induced decreases in T cells and cells of the monocyte/macrophage lineage. In addition, anti-Ang2 enhanced radiation-induced apoptosis in cultured endothelial cells. *In vivo*, combination treatment decreased tumor vasculature and increased tumor necrosis in comparison with tumors treated with monotherapies. These results suggest that a combination of Ang2-blocking antibodies with radiation increases tumor growth inhibition and extends the survival of tumor-bearing mice.

Significance: These findings offer a preclinical rationale for further testing of the use of radiation in combination with Ang2-blocking antibodies to improve the overall outcome of cancer treatment.

Introduction

Almost half of all patients with cancer receive radiotherapy as a curative or palliative treatment. Although radiation is commonly used in the treatment of many types of tumors, for example breast, lung, brain, prostate, and rectal cancers (1), several tumor types show resistance to radiotherapy, compromising treatment efficacy. In addition, radiation sensitivity of the surrounding healthy tissues often limits the use of radiotherapy.

Radiation damages not only tumor cells but also cells forming the tumor microenvironment, including immune and endothelial cells. Previous studies have shown that the radiation-induced vascular damage occurs mostly in immature tumor vessels (2). Low doses of radiation have been shown to stimulate vessel formation (2), whereas high doses of microbeam radiation have been shown to damage preferentially tumor vessels, preserving the normal vasculature (3). The radiation-induced vessel damage increases hypoxia, activating hypoxia-inducible factor 1. This increases the expression of VEGF, which promotes the growth of abnormal vessels in tumors (4, 5).

Tumor vessels are malformed and structurally defective, which leads to their dysfunction, plasma leakage into the tumor stroma, poor tissue perfusion, and compromised tissue oxygenation (6–8). The efficacy of radiation depends on a number of factors, of which, oxygen concentration in the target tissue is important, because radiation produces highly reactive oxygen radicals that cause DNA damage and cell death (9). Hypoxia in tumor tissue counteracts radiotherapy, and the increased interstitial fluid pressure resulting from leaky tumor vessels has been reported to reduce the delivery of cytostatic drugs to the tumors (10, 11). Angiogenesis inhibitors, including inhibitors of VEGF and VEGFRs, and vascular disrupting agents, such as combretastatin, have been tested as modifiers of the tumor vasculature in association with radiotherapy (12). Anti-VEGF agents can improve tumor response to radiation, presumably by normalizing the tumor vasculature, and thereby reducing vascular leak, tumor hypoxia, and radiation resistance (2, 12).

Besides VEGF and its receptors, the endothelial angiopoietin (Ang) growth factors and their Tie receptors regulate physiologic and pathologic angiogenesis and vascular remodeling (13). The constitutively expressed ligand Ang1 acts as a stabilizer of blood vessels (14) and has been shown to protect endothelial cells from radiation-induced apoptosis *in vitro* (15). In contrast, Ang2 is a dual, inducible, and context-dependent autocrine modulator, which is involved in vessel destabilization (13). However, previous findings have indicated that Ang2 protects stressed endothelial cells from apoptosis in several tumor models by activating Tie2, thereby limiting the anti-vascular effects of VEGF inhibition (16, 17).

Tissue hypoxia and proinflammatory signals are known to induce Ang2 expression in endothelial cells (13, 18). Ang2 levels are increased in many types of human tumors, for example in colorectal cancer (13). In some cases, such as in melanoma, non–small cell lung cancer, and

[1]Translational Cancer Medicine Program, University of Helsinki, Helsinki, Finland. [2]iCAN Digital Precision Cancer Medicine Flagship, University of Helsinki, Helsinki, Finland. [3]Wihuri Research Institute, Biomedicum Helsinki, University of Helsinki, Helsinki, Finland.

Note: Supplementary data for this article are available at Cancer Research Online (http://cancerres.aacrjournals.org/).

Current address for J. Högström: Cancer Research Institute, Beth Israel Deaconess Medical Center, Harvard Medical School, Boston, Massachusetts; and current address for S. Das, School of Biological Sciences & Biotechnology, Indian Institute of Advanced Research, Gujarat, India.

Corresponding Author: Kari Alitalo, University of Helsinki, Haartmaninkatu 8 (P.O.Box 63), Helsinki FI-00014 Finland. Phone: 3582-9412-5511; Fax: 3582-9412-5510; E-mail: kari.alitalo@helsinki.fi

Cancer Res 2020;80:2639–50

doi: 10.1158/0008-5472.CAN-20-0497

neuroblastoma, induction of Ang2 expression has been shown to correlate with disease progression (19–21). *In vivo*, a single 10 gray (Gy) dose of radiation increased Ang2 mRNA and protein in brain tissue, while decreasing VEGF, Tie2, and Ang1 levels (22). mAbs that neutralize Ang2 and VEGF tend to normalize tumor blood vessels and inhibit tumor growth (23). In addition to Ang2 blocking, Tie1 deletion has also been shown to decrease tumor growth (24). However, therapeutic efficacy of Ang2-blocking antibodies in clinical use has been so far limited (13, 25, 26).

In this study, we report the discovery that Ang2 blocking in combination with small doses of radiation leads to increased tumor vascular damage and to decreased tumor growth.

Materials and Methods

Mice and tumor models

Eighteen- to 20-week-old male C57BL/6JRj mice from Janvier Labs and the tumor cell lines B16-F0 (a generous gift from Dr. Sirpa Jalkanen, University of Turku, Turku, Finland, in 2012) and MC38-GFP (a generous gift from Dr. Jeffrey Schlom, National Cancer Institute, Bethesda, MD, in 2013) were used for the mouse allograft experiments. Twenty-week-old male and female NOD *scid* gamma mice (NSG; NOD.Cg-Prkdc^{scid} Il2rg$^{tm1/wjl}$/SzJ, 005557) from the Jackson Laboratory were injected with human LS174T cells (a generous gift from Dr. Ragnhild A. Lothe and Dr. Olli Kallioniemi, Institute for Molecular Medicine Finland, Helsinki, Finland, in 2015) in the tumor xenograft experiments. Because of the radiation sensitivity of the NSG mice, they were euthanized 5 days after the last dose of radiation. All experiments were approved by the National Animal Experiment Board in Finland (ESAVI/6306/04.10.07/2016 and ESAVI/7945/04.10.07/2017).

LS174T cells passage 6–10 were cultured in DMEM-F12 (BE04-687F/U1, Lonza), containing penicillin/streptomycin and 10% FBS (S181B-500, Biowest), and MC38-GFP and B16-F0 cells, both in passages 6–10, in DMEM (BE12-707F, Lonza) containing 2-mmol/L L-glutamine (25-005-Cl, Corning), penicillin/streptomycin, and 10% FBS. Cell lines were not authenticated or tested for *Mycoplasma*. For *in vivo* tumor experiments, 1×10^6 tumor cells (passage 6–10) were injected subcutaneously. Tumor growth was monitored by manual measurements with a caliber in mice under inhalation anesthesia (isoflurane). Tumor volume was calculated as length $\times$ width $\times$ thickness in mm^3. Tumor growth time (TGT) represents the time, in days, starting from the first day of treatment until the tumor reached the total volume of 2,500 mm^3 (B16-F0) or 2,000 mm^3 (MC38). Tumor growth delay (TGD) was calculated as: $TGT_{treatment} - TGT_{control\ no\ radiation}$.

Antibody injections and radiation

When the tumors were formed, their volumes were measured and mice were randomized into the different treatment groups according to their tumor size. As reported previously (27, 28), intraperitoneal injections of 10 mg/kg of Ang2-blocking antibody (MEDI3617 or 3.19.3) or isotype control antibody were started 3 days before the first radiation dose. The radiation source was the gamma irradiator OB29/4 (STS, isotype Cs137) at the dose of 1.4 Gy/minute.

Histology and IHC

Hematoxylin and eosin (H&E) staining was used to analyze necrotic areas in tumor sections. IHC stainings were done using antibodies for endomucin (sc-65495, 1:500, Santa Cruz Biotechnology), CD31 (553370, 1:250, BD Pharmingen), smooth muscle actin (αSMA, C6198, 1:500, Sigma-Aldrich), Erg (ab133264, 1:250, Abcam), laminin (RB-082-AO, 1:500, Thermo Fisher Scientific), Glut-1 (07-1401, 1:500, Merck), and Caix (ab15086/ab108351, 1:500, Abcam), followed by Alexa Fluor–conjugated secondary antibodies (Molecular Probes). Deparaffinization employed the xylene substitute (Tissue-Tek, Tissue-Clear, 1466, SAKURA) for 3 $\times$ 5 minutes plus rehydration in an alcohol series (2 $\times$ 100%, 2 $\times$ 96%, 1 $\times$ 70%, and 1 $\times$ 50% for 3 minutes each). After heat-induced epitope retrieval, the sections were blocked for endogenous peroxidase activity using H_2O_2 and for nonspecific binding using TNB (NEL700001KT, PerkinElmer). Primary antibodies were incubated in TNB overnight at +4°C. After TNT washes, the sections were incubated in the appropriate species-specific ImmPRESS Kit (MP-7401, MP-7402, MP-7405, Vector Laboratories) secondary antibodies for 30 minutes, washed with TNT and PBS, treated with AEC for 10 minutes, hematoxylin stained, and mounted with Aquatex (1.08562.0050, Millipore). Images were scanned using 3DHISTECH Pannoramic 250 FLASH II Digital Slide Scanner, and unprocessed digital images were analyzed using Pannoramic 250 Scanner Software. The images were modified to optimize visualization using Fiji software.

Analysis of caspase-3/7–positive cells and cell-cycle phase

Human umbilical vein endothelial cells (HUVEC) passage 6–10 were cultured on 6-well plates coated with gelatin. Twenty-four hours after subculture, the growth medium was replaced with medium supplemented with antibodies (MEDI3617 or isotype control antibody, 2 μg/mL) plus IncuCyte Caspase-3/7 Reagent (4440, 4704, 1:1,000, Essen BioScience) for 15 minutes, followed by radiation with 4 Gy $\times$ 1. Images were taken 24 and 48 hours later with Thermo Fisher EVOS FL Inverted Epifluorescence Microscope. The original images were processed and analyzed using Fiji software. For cell-cycle analysis, HUVECs were cultured for 24 hours in endothelial growth medium supplemented with either anti-Ang2 (MEDI3617) or control antibody, and then radiated with a 4 Gy single radiation dose. On the following day, cells were detached with a brief trypsin treatment (Trypsin-EDTA, 25200056, Thermo Fisher Scientific) and fixed with cold 70% ethanol. After at least 4-hour incubation at −20°C, cells were washed with Hank's Balanced Salt Solution (HBSS, 14175-053, Gibco) + 2% FBS once, treated with 0.1 mg RNase A at +37°C for 30 minutes, and then stained with 20 μg of propidium iodide (PI) for 30 minutes at room temperature. Cells were analyzed with BD Accuri C6 Flow Cytometer, and the cell-cycle phases were determined with FlowJo.

Single-cell RNA-sequencing and data analysis

B16-F0 tumor cells were injected into C57BL/6Jrj mice, and 6 days later, the mice were randomized into the treatment groups. Anti-Ang2 was dosed every 3 days starting from day 6, and 2 Gy daily doses of tumor-focused radiation were given on days 9–11. Five days after the last radiation dose, the mice were euthanized and tumors were harvested for single-cell RNA-sequencing (scRNA-seq). Each sample was pooled from 2–6 tumors. Tumors were dissociated in HBSS (14175-053, Gibco) supplemented with 1 mg/mL collagenase type 1 (LS004196, Worthington), 1 mg/mL collagenase H (11074032001, Roche), 4 mg/mL dispase II (04942078001, Sigma), and 1,000 U/mL benzonase (sc-202391, ChemCruz) for 30 minutes at +37°C, followed by 15-minute incubation with Trypsin-EDTA (25200056, Thermo Fisher Scientific) at +37°C and red blood cell lysis buffer (ACK Lysing Buffer, A1049201, Gibco) for 10 minutes at room temperature. Cells in 0.04% BSA-HBSS were analyzed using the Chromium Single Cell 3′RNA-Sequencing System (10x Genomics) with the Reagent Kit v3 according to the manufacturer's instructions. Multiplex libraries were sequenced on the Illumina NovaSeq 6000 System. The Cell Ranger v 2.1.1 mkfastq and count pipelines (10x Genomics) were used to

demultiplex and convert chromium single-cell 3′ RNA-sequencing barcodes and to read data to FASTQ files and generate aligned reads and gene–cell matrices. Reads were aligned to the mouse reference genome mm10. Seurat R package 3.1.1 was used for quality control, filtering, and analysis of the data. Cells were filtered on the basis of UMI counts and the percentage of mitochondrial genes. Cells with more than 10%–15% of mitochondrial genes were filtered out. The expression matrix was further filtered by removing genes with expression in less than three cells and cells with less than 200 expressed genes. The final dataset was down-sampled to include 2,000 cells per sample. To be able to compare the samples with each other, we performed a principal component analysis to identify shared correlation structures and aligned the dimensions using dynamic time warping. After this, we performed clustering using UMAP and set the resolution at 0.5. The scRNA-seq data has been deposited in the Gene Expression Omnibus under accession number GSE149535.

RNA extraction and qPCR analysis

RNA of dissociated melanoma tumors was extracted with NucleoSpin RNA II Kit (Macherey-Nagel #740955) according to the manufacturer's instructions. Cells for RNA extraction were harvested from the samples used for scRNA-seq. cDNA was synthesized with cDNA Synthesis Kit (Thermo Fischer Scientific #4368814) according to the manufacturer's instructions. Gene expression analysis was performed by qPCR using following primers: *Cd4*_fw: 5′ TAGCAACTCTAAGGTCTCTAAC; *Cd4*_rec: 5′GATAGCTGTGCTCTGAAAA; *Cd8*_fw: 5′CCTTCAGAAAGTGAACTCTAC; and *Cd8*_rev: 5′CCAGATGTAAATATCACGGC. Mouse *Gapdh* was used as a housekeeping gene.

Statistical analyses

For each *in vivo* analysis, data from all mice in a treatment group were pooled, analyzed using the Mann–Whitney test, and presented as mean ± SEM. *In vitro* experiments were repeated two to four times, data were pooled from all experiments, analyzed using the Mann–Whitney test, and presented as mean ± SEM. GraphPad PRISM 7 was used for the statistical analyses. Statistical significance, marked by *P* value *, <0.05; **, <0.005; ***, <0.0005; ****, <0.0001, is indicated in the figure legends.

Results

Ang2 is critical for the survival of endothelial cells after radiation

Because Ang2 has been shown to have a protective role in stressed endothelial cells (16), we speculated that Ang2 could also be critical for the survival of endothelial cells after radiation. To test this, we exposed cultured HUVECs to 2 Gy dose of radiation on 2 consecutive days and analyzed *ANG2* RNA 24 hours after radiation. Although radiation increased *ANG2* RNA only slightly, radiation in combination with Ang2 blocking increased *ANG2* RNA very significantly, reflecting stress in the endothelial cells induced by this combination treatment (**Fig. 1A**). To study the possible effect of Ang2 on endothelial cell survival after radiation, we next supplemented the endothelial growth medium with Ang2-blocking (MEDI3617) or isotype control antibody, plus the IncuCyte Caspase-3/7 reagent, radiated the cultures with single dose of 4 Gy radiation, and 24 and 48 hours thereafter, determined the percentage of caspase-3/7–positive apoptotic cells. We found that the combination caused significantly more apoptosis than either treatment alone (**Fig. 1B**). However, γH2AX staining for detection of DNA damage did not indicate differences between radiation- and anti-Ang2 plus radiation–treated HUVECs, indicating that Ang2 blocking does not sensitize endothelial cells to radiation-induced DNA damage (**Fig. 1D**; Supplementary Fig. S1A). To analyze how the combination treatment affects endothelial cell proliferation, HUVECs were treated for 24 hours with the antibodies and subjected to a 4 Gy radiation dose, followed by staining for the Ki67 on the next day. The results showed that the anti-Ang2 plus radiation–treated cultures had more cells in the G_0-phase (Ki67 negative) than cultures treated with either radiation or antibodies alone (**Fig. 1C** and **D**). This result was further supported by flow cytometry analysis of PI-stained HUVECs, which showed that there were more endothelial cells in the G_0–G_1 cell-cycle phase in the combination-treated cultures than in the other cultures (**Fig. 1E**; Supplementary Fig. S1B–S1E). These results indicated that anti-Ang2 increases radiation-induced endothelial cell-cycle arrest and cell death.

Low doses of radiation in combination with Ang2 blocking inhibit melanoma tumor growth

To test whether Ang2 blocking plus radiation-induced endothelial cell death could lead to tumor growth inhibition, we tested the effect of combination treatment in subcutaneous B16-F0 melanoma allografts in C57BL/6JRj mice. Anti-Ang2 (MEDI3617) injections were started 5 days after the tumor cell implantation and then continued every 3 days, and whole-body radiation was given on days 8–10, when the tumors had grown to an average size of 140 mm^3. Three daily doses of 2 Gy whole-body radiation induced only a trend of tumor growth inhibition (**Fig. 2A**). This effect was of similar magnitude as the effect of anti-Ang2 antibodies (**Fig. 2A**). Although the monotherapies did not show significant tumor growth inhibition, the tumor-bearing mice subjected to a combination treatment with anti-Ang2 plus radiation showed a significant improvement of tumor growth inhibition (**Fig. 2A**).

Anti-Ang2 treatment combined with radiation extends the survival of melanoma tumor–bearing mice

To test the long-term effects of the combined anti-Ang2 plus radiation treatment, the B16-F0 allografts in the four treatment groups were allowed to grow until they reached a total tumor volume of 2,500 mm^3, when the mice were euthanized. However, because the tumors in the combination treatment group did not seem to progress to meet the euthanization criteria, antibody treatment was discontinued on day 44, when all mice in the other treatment groups had already been euthanized. The termination of Ang2 antibody treatment accelerated tumor growth in the combination treatment group, and by day 63, all tumor volumes in the combination treatment group had reached a volume of 2,500 mm^3 (**Fig. 2B** and **D**). The TGD in the anti-Ang2 monotherapy group was on average 5 days, in the radiation monotherapy group 13 days, and in the combination treatment group 34 days (**Fig. 2C**).

We then repeated the experiment by starting the anti-Ang2 (MEDI3617) antibody treatment on day 3 after tumor implantation, when the tumor volume was about 15 mm^3 on average, and whole-body radiation was given on days 6–8. In this experiment, the antibodies were injected every fourth day. Although both monotherapies resulted in a significant tumor growth inhibition, the combination treatment again significantly improved both tumor growth inhibition and host survival (**Fig. 2E–H**). Notably, anti-Ang2 treatment (i) given only 3 days before radiation and on first radiation day, (ii) starting on the first radiation day, or (iii) starting on following day of last radiation dose resulted in shorter survival than our standard combination treatment (Supplementary Fig. S2A–S2D). We conclude that for

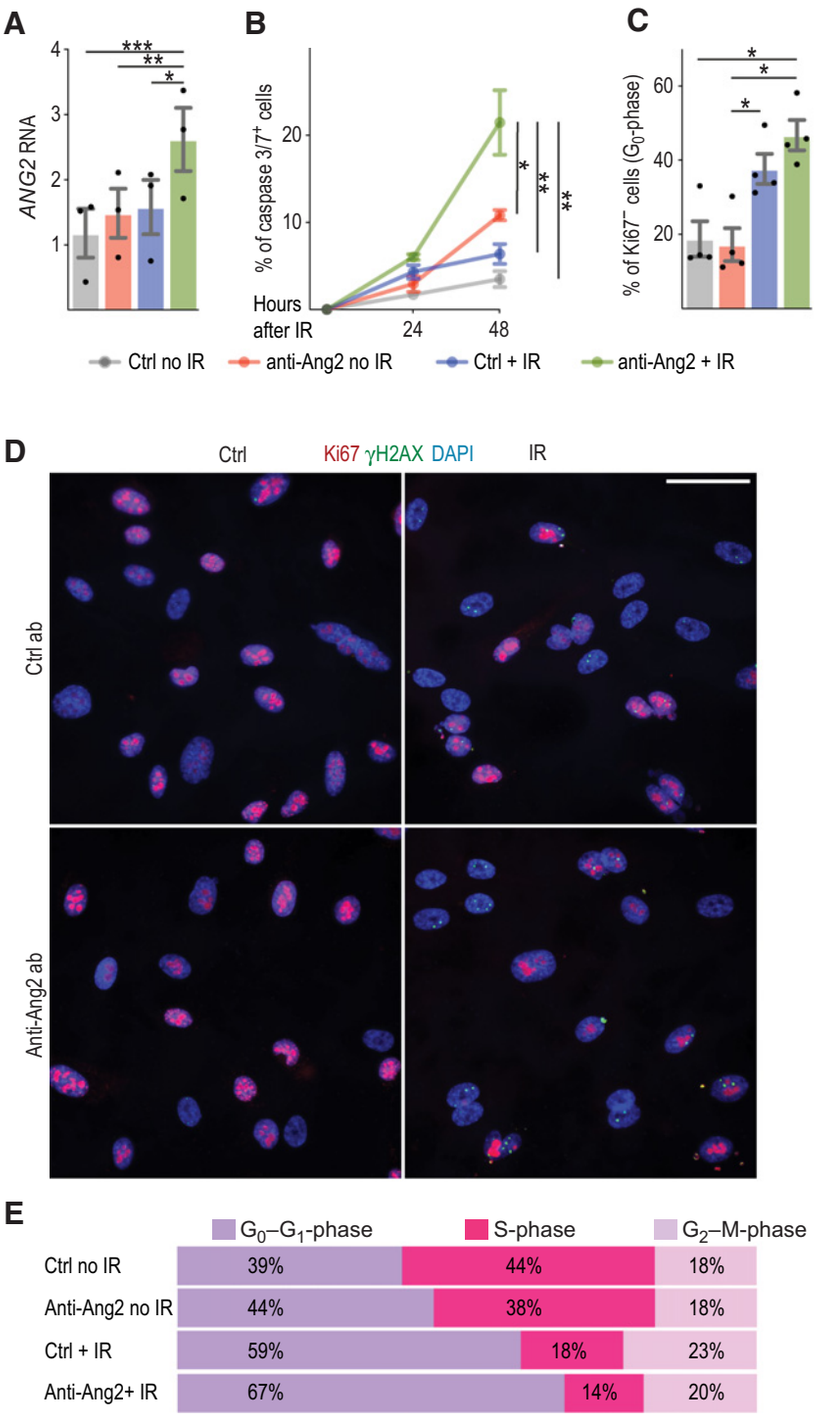

Figure 1.

Ang2 is critical for endothelial cell survival after radiation (IR)-induced damage. **A** and **B,** HUVECs were plated and allowed to grow for 24 hours, after which, growth medium was replaced and anti-Ang2 (MEDI3617) or isotype control antibody (2 μg/mL) was added. Fifteen minutes later, the cells were either sham-radiated or radiated with either 2 Gy × 1 (**A**) or 4 Gy × 1 (**B**). On the following day, the cells were again either sham-radiated or radiated with 2 Gy × 1 (**A**). *ANG2* RNA was measured in three replicate experiments 24 hours after the last radiation dose. **B,** The percentage of caspase-3/7–positive HUVECs was analyzed 24 and 48 hours after 4 Gy radiation. **C–E,** HUVECs were plated, allowed to grow for 24 hours in growth medium supplemented with either anti-Ang2 (MEDI3617) or isotype control antibody (ab; 2 μg/mL), and then radiated with 4 Gy × 1. On the following day, cells were stained for either Ki67 or PI. The percentage of Ki67-negative cells was counted from four replicate experiments (**C** and **D**), and the cell-cycle phase was analyzed from PI staining and flow cytometry (**E**). Mean ± SEM for each treatment group and for each cell-cycle phase: control (ctrl) no IR: G_0–G_1-phase 39 + 4, S-phase 44 + 6, and G_2–M-phase 18 + 2; anti-Ang2 no IR G_0–G_1-phase 44 + 3, S-phase 38 + 1, and G_2–M-phase 18 + 2; ctrl + IR G_0–G_1-phase 59 + 11; S-phase 18 + 5, and G_2–M-phase 23 + 15; and anti-Ang2 + IR G_0–G_1-phase 67 + 12, S-phase 14 + 1, and G_2–M-phase 20 + 11 (**E**). *, $P < 0.05$; **, $P < 0.005$; ***, $P < 0.0005$. Scale bar, 50 μm.

optimal results, anti-Ang2 treatment should be started before radiation and continued thereafter.

Additive effect of anti-Ang2 and radiation in colorectal allografts

To study whether the effect of the combination treatment could be reproduced in another tumor type, we next analyzed growth of subcutaneous MC38 colorectal carcinoma allografts subjected to the treatments. To independently confirm our findings, we further used another monoclonal Ang2-blocking antibody (3.19.3; ref. 28). The Ang2-blocking antibodies were injected every third day starting on day 8, when the tumor volume was 25 mm^3 on average, and 2 Gy whole-body radiation doses were given on days 11–13. Radiation monotherapy strongly suppressed MC38 allograft growth and increased the survival of the tumor-bearing mice, whereas anti-Ang2 monotherapy resulted only in a trend of slower tumor growth (**Fig. 3A–D**). Yet, the

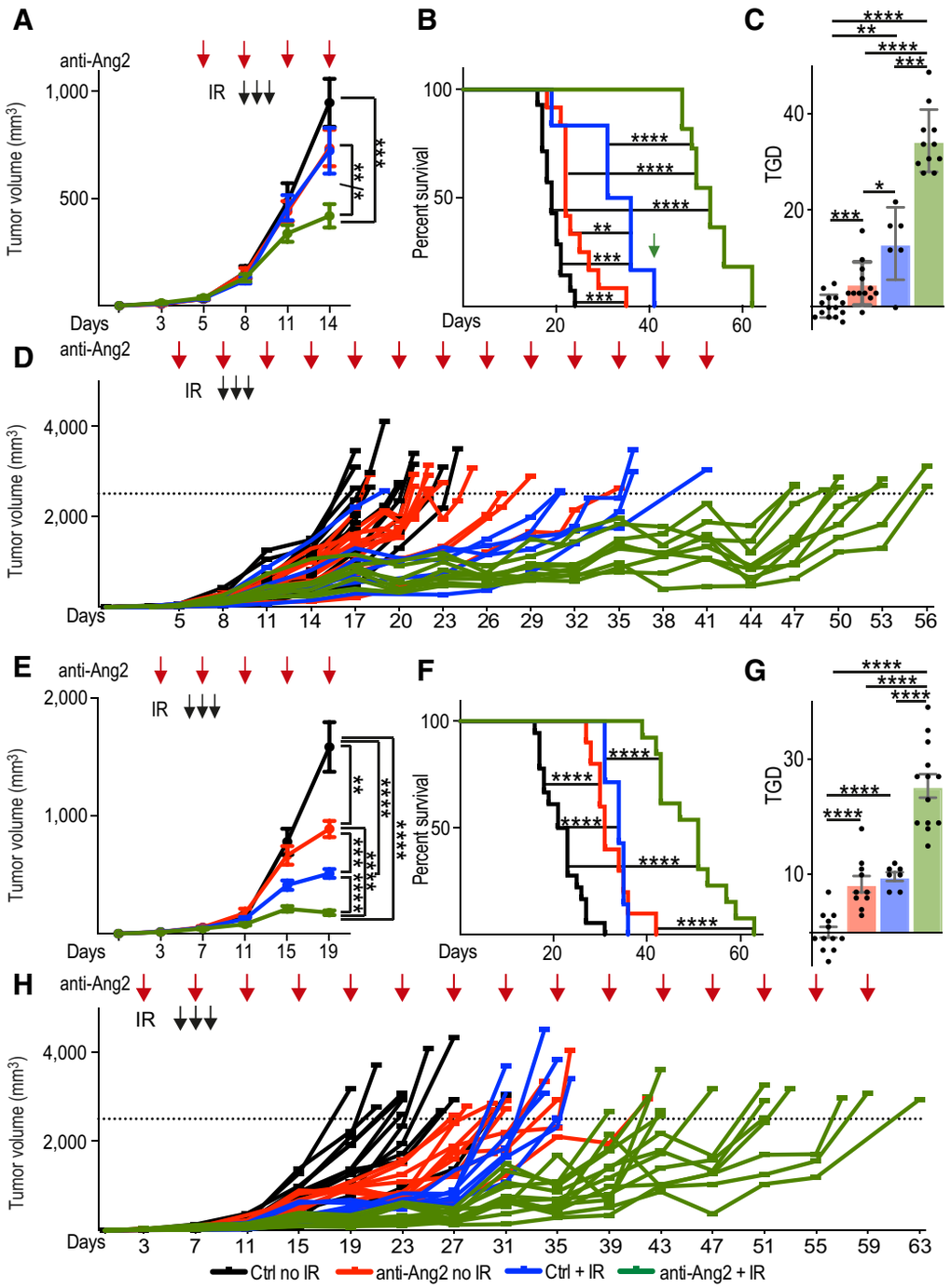

Figure 2.

Increased melanoma growth inhibition and extended survival in mice treated with a combination of Ang2-blocking antibodies and a small dose of radiation. B16-F0 melanoma cells were injected subcutaneously into C57BL/6Jrj mice. Anti-Ang2 (MEDI3617) or control antibody (red arrows) was injected either every third day starting from day 5 after the implantation of tumor cells, until the indicated timepoint (green arrow, day 41; **A**–**D**), or every fourth day starting from day 3 after the implantation of tumor cells (**E**–**H**). The mice received a total of 6 Gy whole-body radiation (IR; black arrows) in three equal fractions on days 8, 9, and 10 (**A**–**D**) or on days 6, 7, and 8 (**E**–**H**). Mice were euthanized when the total tumor volume reached 2,500 mm^3. **C** and **G,** TGD (compared with control no IR treatment group) was calculated for each treatment group. Number of mice per group: control (ctrl) no IR, 14; anti-Ang2 no IR, 12; control + IR, 6 and anti-Ang2 + IR, 11 (**A**–**D**); and control no IR, 12; anti-Ang2 no IR, 10; control + IR, 7; and anti-Ang2 + IR, 13 (**E**–**H**). *, $P < 0.05$; **, $P < 0.005$; *** P, < 0.0005; ****, $P < 0.0001$.

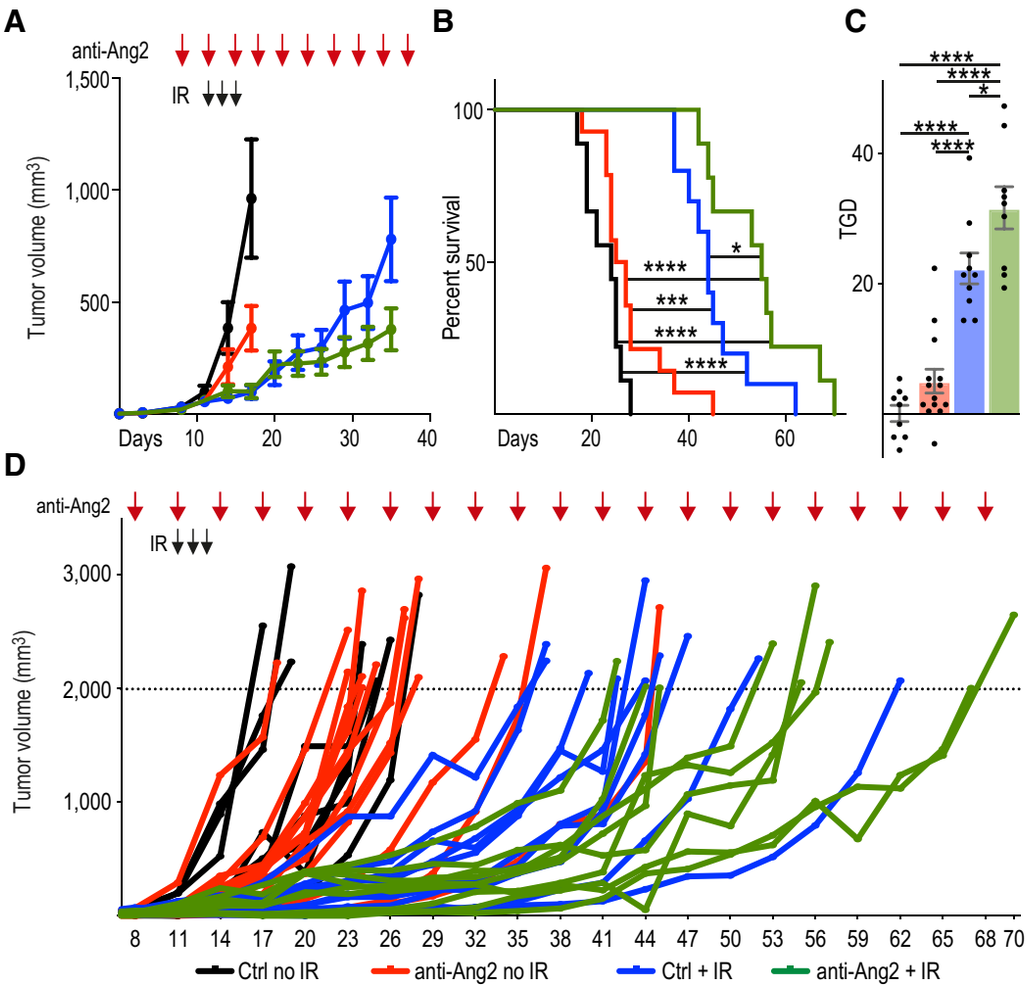

Figure 3.

Colorectal carcinoma tumor growth inhibition and extended survival in mice treated with anti-Ang2 plus radiation. MC38 colorectal carcinoma cells were injected subcutaneously into C57BL/6Jrj mice. Anti-Ang2 (clone 3.19.3) or control antibody (red arrows) was given every third day starting on day 8 after the implantation of the tumor cells until the end of the experiment. The mice received a total of 6 Gy whole-body radiation in three equal fractions on days 11, 12, and 13 (black arrows). The mice were euthanized when the total tumor volume reached 2,000 mm^3. **A,** Tumor growth was measured every 3 days starting on day 8. The figure shows the tumor growth curves in each treatment group until the first mouse was euthanized from nonradiated (black and red) and radiated (blue and green) treatment groups. **B,** Survival of the mice. **C,** TGD compared with control (ctrl) no radiation (IR) group. **D,** All individual tumor growth curves. Number of mice per group: control no IR, 9; anti-Ang2 no IR, 14; control + IR, 10; and anti-Ang2 + IR, 9. *, $P < 0.05$; ***, $P < 0.0005$; ****, $P < 0.0001$.

combination treatment with anti-Ang2 plus radiation significantly increased host survival when compared with the monotherapies (**Fig. 3B** and **C**). The TGD in the anti-Ang2 monotherapy group was on average 5 days, in the radiation monotherapy group 22 days, and in the combination treatment group 32 days (**Fig. 3C**).

Effect of the combination treatment in severely immunodeficient mice

Recent research has indicated that the results of chemotherapy often depend on the adaptive immune response, whereas in the case of radiotherapy its role is less clear (29, 30). To investigate whether the inhibitory effect of Ang2 blocking in combination with radiation works in severely immunodeficient mice, we injected LS174T cells subcutaneously and allowed the tumors to develop to an average volume of 135 mm^3 (day 16), after which, the mice were injected with anti-Ang2 (MEDI3617) or control antibody every third day. Because of the high sensitivity of the NSG mice to radiation, only a 0.5 Gy radiation dose was administered daily over 4 consecutive days starting on day 19. We found that radiation and anti-Ang2 monotherapies decreased tumor growth. The combination treatment significantly increased tumor growth inhibition in the first experiment, but in a repeated experiment only a trend of additional inhibition was found (Supplementary Fig. S3A–S3F). This suggested that adaptive immunity may improve the outcome of the combination treatment.

Anti-Ang2 improves tumor growth inhibition in response to focused radiation

We next tested whether the results obtained with whole-body radiation plus anti-Ang2 could be reproduced with tumor-focused radiation (TF-IR). B16-F0 allografts (~80 mm^3) in otherwise lead-shielded mice were radiated with a 2 Gy daily dose on days 12–14. Anti-Ang2 (MEDI3617) injections were started 3 days before the first

radiation dose, and were continued every 3 days. The results showed that TGD in anti-Ang2 and radiation monotherapy groups was 1 and 2 days, respectively, whereas the delay was 13 days in the combination treatment group, indicating that TF-IR increases tumor growth inhibition by anti-Ang2 highly significantly (Supplementary Fig. S4A–S4D). Similar results were obtained in a repeated experiment: anti-Ang2 monotherapy, radiation monotherapy, and the combination treatment–induced TGDs were 6, 3, and 18 days, respectively (Supplementary Fig. S4E–S4H). Thus, the mice treated with the combination therapy lived on average 4–6 times longer than mice treated with either monotherapy, even when tumor TF-IR was used.

Ang2 blocking does not sensitize mice to radiation-induced adverse effects

To analyze possible adverse effects of the combination treatment, the wellbeing of the mice was regularly monitored during the experiments. Although one of the most sensitive tissues to radiation-induced damage is the intestine, none of the mice developed diarrhea in any of the experiments. Furthermore, the reduction in body weight in the mice treated with the combination treatment did not significantly differ from that in mice treated with radiation monotherapy 7 or 10 days after the last dose of radiation (Supplementary Fig. S5A–S5F). In the whole-body radiation experiments, 7% (3/44) of the radiation monotherapy treated mice and 2% (1/54) of the combination treated mice had to be euthanized on the basis of decreased body weight (>20%), whereas none of the mice that received TF-IR met the euthanization criteria. These results indicated that Ang2 blocking did not sensitize the mice to major radiation-induced adverse effects.

Radiation increases vascular pruning induced by anti-Ang2

To see whether the combination treatment had affected the tumor vasculature, as expected on the basis of the *in vitro* experiments, we studied the tumor blood vessels by immunostaining endothelial cells (endomucin plus CD31), pericytes (NG2), and smooth muscle cells (αSMA). Consistent with previous findings (27, 31), the pericyte and smooth muscle cell coating of tumor vessels was increased by anti-Ang2 in the LS174T and B16-F0 tumors when analyzed 5 days after the last radiation dose (Supplementary Fig. S6A–S6D). The vascular analysis further indicated that both anti-Ang2 and radiation monotherapy decreased vascular density in the LS174T and B16-F0 tumors, and that the effect of the combination treatment was significantly stronger than the effect of the monotherapies 5 days after the last dose of radiation (**Fig. 4A–C**). Staining of the endothelial Erg protein and basement membrane laminin confirmed that the combination treatment led to increased loss of vascular endothelium from the tumors (Supplementary Fig. S6E–S6J). A similar effect of the combination treatment was observed in the B16-F0 and MC38 tumors harvested at the experimental endpoint (**Fig. 4D–F**).

Anti-Ang2 treatment rescues radiation-induced loss of inflammatory cells

To analyze the tumor microenvironment in mice treated with TF-IR plus anti-Ang2, B16-F0 tumor cells were injected into C57BL/6Jrj mice, and 6 days later, the mice were randomized to the treatment groups. Anti-Ang2 was dosed every 3 days starting from day 6, and 2 Gy daily doses of TF-IR were given on days 9–11. Five days after the last radiation dose, the mice were euthanized and tumors were harvested for scRNA-seq (**Fig. 5A**). ScRNA-seq analysis of 2,000 cells per treatment group revealed less $Cd4^+$ and $Cd8^+$ T cells and cells of the monocyte/macrophage lineage in the TF-IR group than in the non-radiated groups, but not in the combination treatment group (**Fig. 5B** and **C**; Supplementary Fig. S7D). qPCR from total RNA was consistent with the rescue of the radiation-induced decrease of the Cd4 and Cd8 T cells in the combination treatment group (Supplementary Fig. S7A and S7B). These results indicated that Ang2 blocking protects T cells and monocytes/macrophages from radiation-induced damage. ScRNA-seq analysis also revealed that endothelial Ang2 expression was higher in all the treatment groups than in the control group, with highest levels in the combination-treated group (Supplementary Fig. S7C).

Increased necrosis in the combination-treated tumors

To analyze whether anti-Ang2 treatment led to increased tumor tissue hypoxia before radiation, we injected pimonidazole intraperitoneally to the tumor-bearing mice, and stained pimonidazole-thiol adducts of hypoxic cells in the tumor sections. As additional markers of hypoxia, we stained for the hypoxia-inducible proteins carbonic anhydrase IX (Caix) and glucose transporter 1 (Glut1). In tumors isolated before radiation, there was no significant difference in the pimonidazole-thiol adducts, Caix, or Glut1 expression between control and anti-Ang2 antibody–treated B16-F0 allografts in either of two different experiments, indicating that the blocking of Ang2 did not increase tumor hypoxia before radiation (Supplementary Fig. S8A and S8D). ScRNA-seq analysis of the B16-F10 tumors 5 days after the radiation showed that the hypoxia markers *Caix* and *Glut1* were expressed in a greater fraction of tumor cells in the TF-IR monotherapy group than in the other treatment groups. This indicated again that Ang2 blocking rescued radiation-induced hypoxia in the melanoma cells (Supplementary Fig. S8B and S8C). This may be due to the decrease of oxygen consumption after cell death in the combination treatment group, because H&E stainings showed either a trend or significantly more necrosis in the combination treatment group than in the other treatment groups 5 days after radiation and at mouse termination time points (**Fig. 6A–F**).

Discussion

On the basis of our results, Ang2 seems to have a protective function against radiation-induced endothelial cell damage, and when Ang2 is blocked, radiation leads to enhanced vascular pruning, thus resulting in increased tumor growth inhibition. This effect of the combination treatment was evident in all three tumor models used, and it was associated with increased host survival in both melanoma and colorectal carcinoma models. Importantly, increased survival was also observed in the combination-treated group when TF-IR was used.

Although we did not detect significantly increased hypoxia before radiation or 5 days after the last radiation dose in the tumor cells, the anti-Ang2 plus radiation–treated tumors were more necrotic than tumors in the other treatment groups 5 days after the radiation and at mouse termination. It is possible that our analysis at the selected time points does not allow for detection of transient hypoxia upon decrease of tumor vasculature, but in such cases, the hypoxia may be rapidly compensated for by the simultaneous increase in tumor cell death that decreased tumor oxygen consumption.

In our experiments, the anti-Ang2 plus radiation-induced decrease of the tumor vasculature was evident both 5 days after the last dose of radiation and at the endpoint of the survival experiments. We found that Ang2 activity was critical for endothelial cell survival also in culture, because the anti-Ang2–treated endothelial cells showed more apoptosis and less proliferating cells after radiation than the cultures treated with radiation only. Previous studies have indicated that Ang2 can act as an autocrine endothelial survival factor in stressed

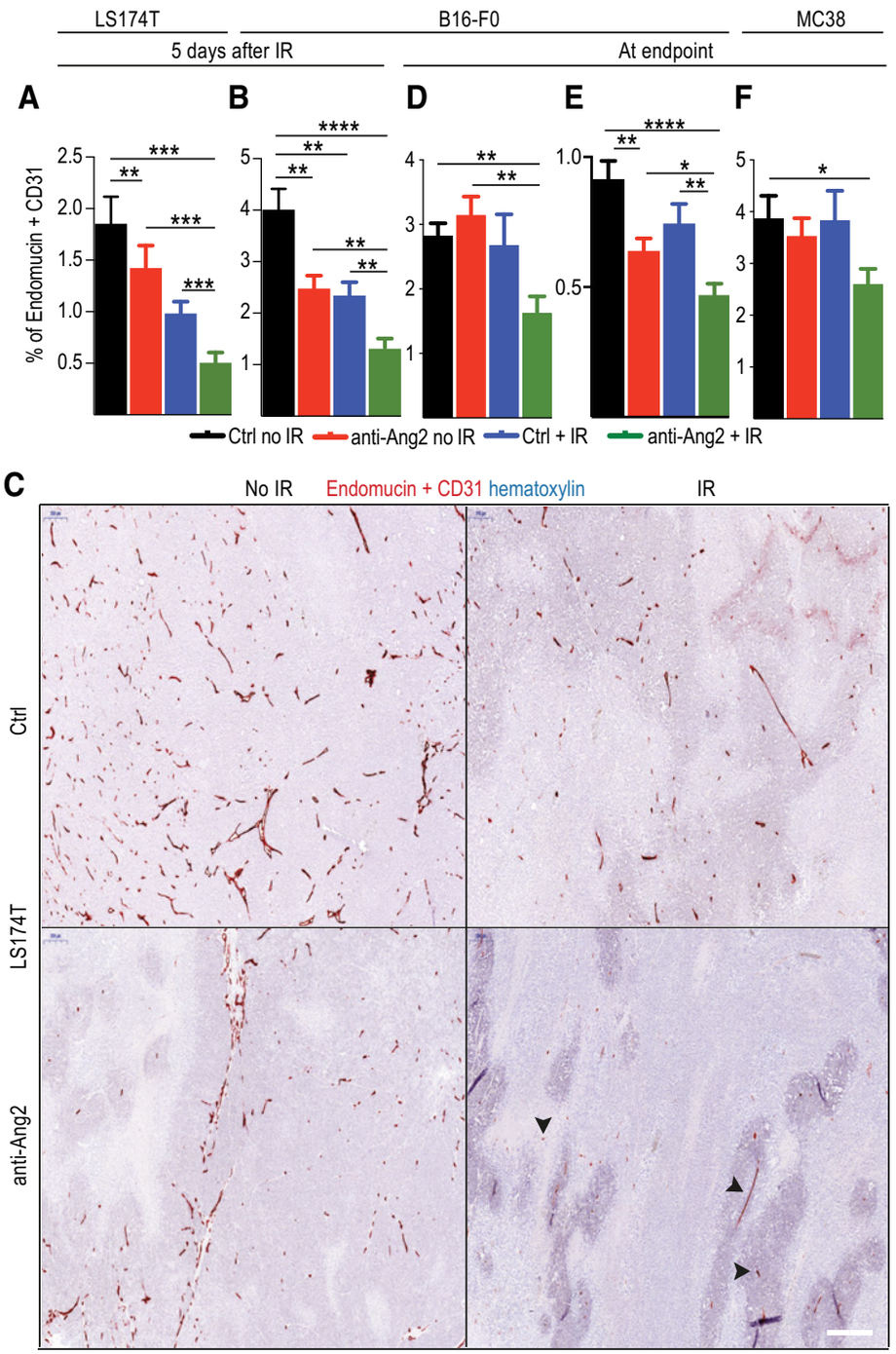

Figure 4.
Quantification of tumor vessels in mice treated with anti-Ang2 plus radiation (IR). **A** and **B,** Five days after the last fraction of radiation, mice were euthanized. Tumor sections were stained for endomucin and CD31, and the endothelial area was quantified. **C,** Representative images from LS174T tumor sections stained for endomucin plus CD31. Arrowheads point to the few remaining capillaries in the combination-treated tumor sections. Scale bar, 0.4 mm. **D–F,** Quantification of endomucin plus CD31 staining area in B16-F0 and MC38 tumors after mouse euthanization. *, $P < 0.05$; **, $P < 0.005$; ***, $P < 0.0005$; ****, $P < 0.0001$. Ctrl, control.

conditions (16), an activity that the Ang2 antibodies likely neutralized in the tumor-bearing mice and in cultured endothelial cells.

To improve the overall outcome of cancer therapy, radiation sensitizers have been tested that not only increase the local tumor cell death induced by radiation, but also induce tumor cell death in distant metastases (32). Most of the radiation sensitizers used so far have been chemotherapeutic agents, which reduce proliferating cells in both normal and tumor tissues by inducing DNA damage, inhibiting DNA repair, promoting cell-cycle arrest, or apoptosis and reoxygenation (33). Furthermore, preclinical studies in which radiation was combined with immune checkpoint blockade have shown promising abscopal effects (34, 35). Several preclinical studies have indicated that VEGF-blocking agents combined with radiation can provide additive inhibition of growth in human and murine tumor models (36, 37). Such a concept has been advanced to clinical trials, but it has not yet led to clinical applications (2), although the anti-VEGF antibody plus radiation treatment was well tolerated in both preclinical and in clinical studies (2, 38). In our

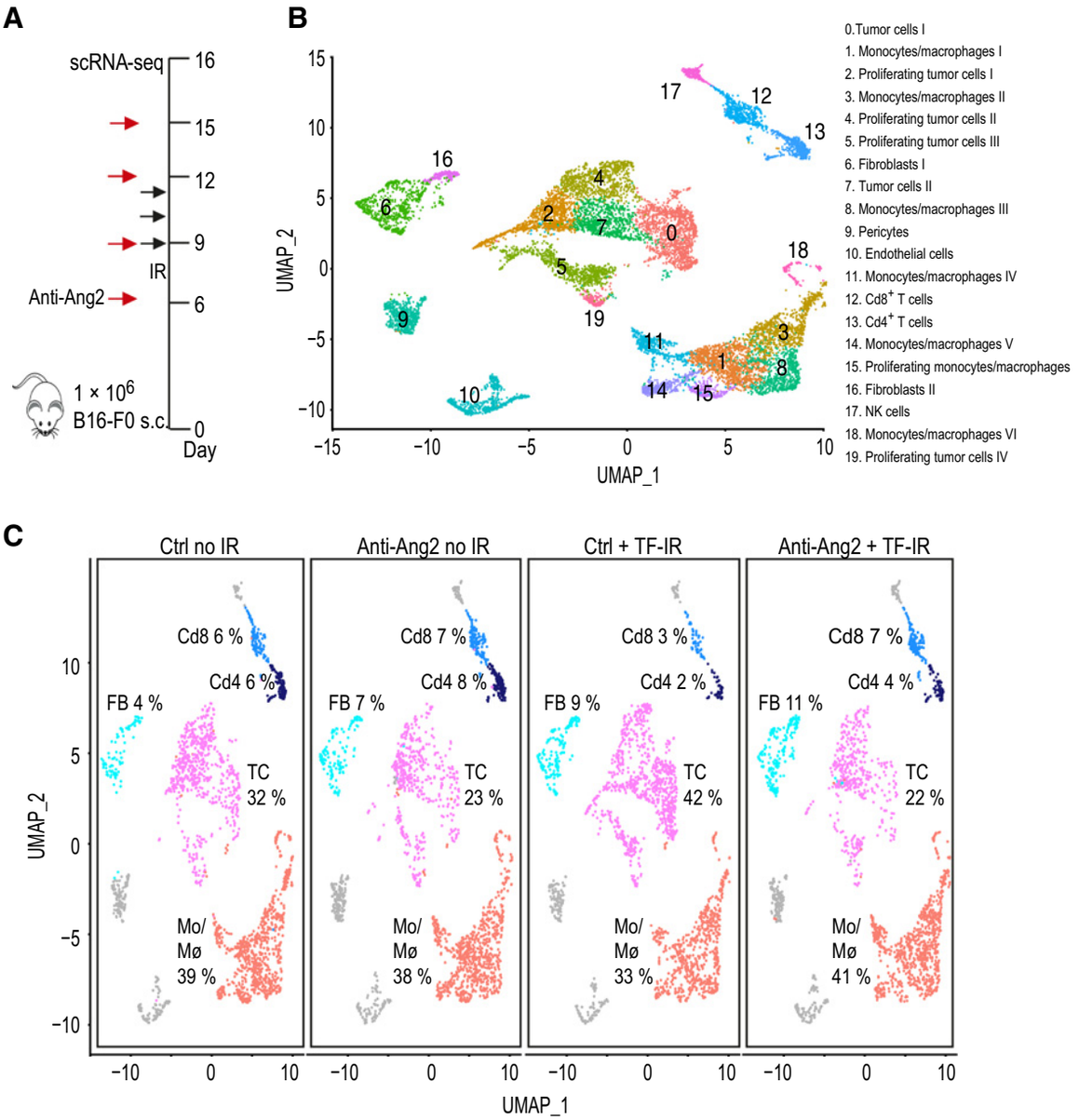

Figure 5.

Ang2 blocking inhibits radiation (IR)-induced decrease of T cells and cells of the monocyte/macrophage lineage. **A–C,** B16-F0 cells were injected subcutaneously into C57BL/6Jrj mice. After randomizing of the mice into different treatment groups on day 6, anti-Ang2 injections were started and continued every 3 days. Daily radiation doses of 2 Gy were given on days 9–11. The mice were euthanized and tumors were harvested for scRNA-seq analysis on day 16. **B**, Cell populations based on single-cell RNA clusters. **C,** Percentages of $Cd8^+$ and $Cd4^+$ T cells, fibroblasts (FB), tumor cells (TC), and monocytes/macrophages (Mo/Mø) in the treatment groups. Number of tumors per treatment group: control (ctrl) no IR, 6; anti-Ang2 no IR, 6; control + TF-IR, 2; and anti-Ang2 + TF-IR, 6. NK cells, natural killer cells.

experiments, blocking Ang2 in combination with small doses of radiation increased the survival of the tumor-bearing mice. Because the blocking of Ang2 has been shown to decrease tumor growth and metastasis in mouse tumor models (31), combining anti-Ang2 treatment with radiation could inhibit tumor growth not only in primary tumors but also in metastases.

Besides anti-VEGF treatments, also drugs targeting the Tie2 signaling pathway have also been tested to improve the effect of radiotherapy (39). Goel and colleagues showed that pretreatment with vascular endothelial protein tyrosine phosphatase (VE-PTP) inhibitor, which increases the activation of Tie2, decreased breast carcinoma tumor growth and increased tumor doubling time by 2.5 days after a single radiation dose of 20 Gy (39). In our experiments, anti-Ang2–blocking antibodies in combination with radiation delayed tumor growth in a colorectal carcinoma model by 10 days and in a melanoma model on average by 16 days, when compared with

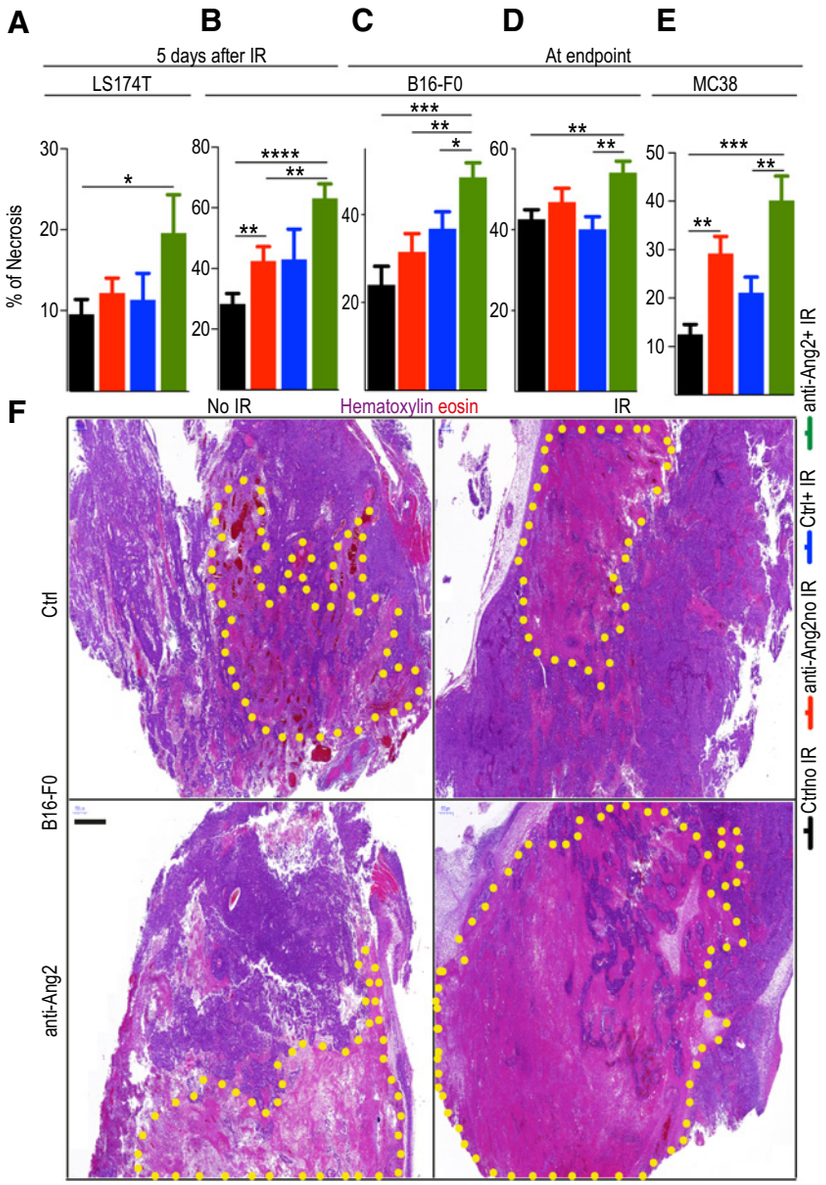

Figure 6.

Anti-Ang2 treatment combined with radiation (IR) increases tumor necrosis. **A** and **B,** Five days after the last fraction of whole-body radiation, the mice bearing the indicated tumors were euthanized and tumor sections were stained with H&E. Quantification of tumor necrosis in LS174T (**A**) and B16-F0 (**B**) tumors. **C–F,** B16-F0 and MC38 allografts excised at experiment endpoint were stained with H&E. Quantification of tumor necrosis in B16-F0 allografts after whole-body radiation (**C** and **F**) or after TF-IR (**D**) and in MC38 allografts treated with whole-body radiation (**E**). **F,** Representative images of B16-F0 tumor sections stained with H&E. Yellow dots encircle the main necrotic areas. Scale bar, 1 mm. *, $P < 0.05$; **, $P < 0.005$; ***, $P < 0.0005$; ****, $P < 0.0001$. Ctrl, control.

radiation monotherapy–induced delay in tumor growth. This indicates that even very small doses of radiation can reduce tumor growth when combined with the anti-Ang2–blocking treatment. This could be beneficial in the treatment of patients with cancer because the side effects of radiation on healthy tissue in the radiation field often limit the radiation dose. Anti-Ang2 could perhaps allow for the use of lower radiation doses, with less side effects and increased tumor growth inhibition.

Currently, there is strong interest in new drug combinations that lead to "synthetic lethality" of tumor cells (40), and this especially concerns pathways that interact with the antitumor immune responses. Ang2 serum concentrations have been shown to predict poor survival of patients receiving CTLA4 or PD1 immune checkpoint–blocking antibodies, both of which increase Ang2 levels in serum (41). In their article, Schmittnaegel and colleagues showed that dual Ang2 and VEGF inhibition in combination with the anti-PD-1 immune checkpoint inhibitor results in improved tumor growth control (42). The authors concluded that immune cells are essential in determining the outcome of antiangiogenic treatments. In our experiments, both the Ang2-blocking antibody and TF-IR increased endothelial Ang2 expression *in vivo*, with an additive effect in the combination treatment group. In addition, at the same time, the blocking antibody inhibited the TF-IR–induced decrease in the tumor infiltrating T cells, especially $Cd8^+$ T cells, and monocytes/macrophages, supporting the findings of Schmittnaegel and colleagues (42).

Reasons for the increased recruitment of immune cells to the tumors likely include immune-attracting signals induced by the increased tissue damage in the combination-treated tumors and subsequent vascular normalization 5 days after the radiation in the anti-Ang2 monotherapy and anti-Ang2 plus IR treatment groups. In addition, the TF-IR decreases radiation-induced damage to the bone marrow

compared with the whole-body radiation, which further enables the recruitment of immune cells to the tumors. The combination treatment also showed some signs of efficacy in NSG mice, which represent the most immune-compromised xenograft model available. Of note, one of the mutations in the NSG mice inhibits the non-homologous end joining DNA repair mechanism, and this sensitizes them to radiation-induced damage. Our results indicated that the blocking of Ang2 may also increase the efficacy of radiotherapy in these conditions, making it possible that it could work even in the absence of adaptive immunity.

On the basis of our results, the anti-Ang2 plus radiation treatment should be further tested in transgenic and patient-derived xenograft tumor models, and if successful, in a clinical trial. Furthermore, anti-PD-1/PD-L1 could be tried for the improvement of the efficacy of the treatment with Ang2-blocking antibodies plus radiation, especially because the combination treatment increased tumor infiltration by the cytotoxic $Cd8^+$ T cells and because previous studies have shown synergistic effects when antiangiogenic treatment has been combined with immune checkpoint therapies (43).

Disclosure of Potential Conflicts of Interest

No potential conflicts of interest were disclosed.

Authors' Contributions

Conception and design: P. Kallio, E. Jokinen, S. Das, K. Alitalo
Development of methodology: P. Kallio, E. Jokinen, S. Das, K. Alitalo
Acquisition of data (provided animals, acquired and managed patients, provided facilities, etc.): P. Kallio, E. Jokinen, J. Högström, S. Das, S. Heino, M. Lähde, J. Brodkin, E.A. Korhonen
Analysis and interpretation of data (e.g., statistical analysis, biostatistics, computational analysis): P. Kallio, E. Jokinen, K. Alitalo
Writing, review, and/or revision of the manuscript: P. Kallio, K. Alitalo
Administrative, technical, or material support (i.e., reporting or organizing data, constructing databases): P. Kallio, S. Heino, K. Alitalo
Study supervision: K. Alitalo

Acknowledgments

This work was funded by the iCAN Digital Precision Cancer Medicine platform (grant 320185), Academy of Finland (grants 292816, 273817, 312516, and 320249), the Centre of Excellence Program 2014–2019 (grant 307366), the Cancer Foundation Finland, the Sigrid Jusélius Foundation, The Southern Finland Regional Cancer Center FICAN South, the Hospital District of Helsinki, Uusimaa Research Grants, Helsinki Institute of Life Sciences (HiLIFE), and Biocenter Finland (all to K. Alitalo), the Cancer Foundation of Finland, The Finnish Medical Foundation, the Maud Kuistila Memorial Foundation, the Magnus Ehrnrooth Foundation, Mary and Georg C. Ehrnrooth Foundation, the Biomedicum Helsinki Foundation, and Finnish Cultural Foundation (all to P. Kallio). We thank Dr. Sirpa Jalkanen for the B16-F0 cell line, Drs. Ragnhild A. Lothe and Olli Kallioniemi for the LS174T cell line, Dr. Jeffrey Schlom for the MC38-GFP cell line, MedImmune Inc. for the anti-Ang2 antibodies, Drs. Lauri Eklund, Marikki Laiho, Curzio Rüegg, Tuomas Tammela, Ruth Muschel, and Valentin Djonov for comments on the article, and Tanja Laakkonen, Riitta Kauppinen, David He, Katja Salo, and Tapio Tainola for their help with the experiments. The Biomedicum Imaging Unit is acknowledged for microscopy services, the Genome Biology core facility supported by HiLIFE and the Faculty of Medicine, University of Helsinki, and Biocenter Finland for scanning of tumors sections, the HiLife Flow Cytometry Unit, University of Helsinki for flow cytometry analysis, the Laboratory Animal Center of the University of Helsinki for expert mouse husbandry, and FIMM Single-Cell Analytics unit supported by HiLIFE and Biocenter Finland for single-cell sequencing services.

The costs of publication of this article were defrayed in part by the payment of page charges. This article must therefore be hereby marked *advertisement* in accordance with 18 U.S.C. Section 1734 solely to indicate this fact.

Received February 13, 2020; revised March 26, 2020; accepted April 13, 2020; published first April 20, 2020.

References

1. Joiner M, van der Kogel A, Steel GG. Introduction: the significance of radiobiology and radiotherapy for cancer treatment. In: Basic clinical radiobiology. 2009. London: Hodder Arnold. p.1–3.
2. Kleibeuker EA, Griffioen AW, Verheul HM, Slotman BJ, Thijssen VL. Combining angiogenesis inhibition and radiotherapy: a double-edged sword. Drug Resist Updat 2012;15:173–82.
3. Bouchet A, Serduc R, Laissue JA, Djonov V. Effects of microbeam radiation therapy on normal and tumoral blood vessels. Phys Med 2015;31:634–41.
4. Ahluwalia A, Tarnawski AS.Critical role of hypoxia sensor - HIF-1a in VEGF gene activation. implications for angiogenesis and tissue injury healing. Curr Med Chem 2012;19:90–7.
5. Forsythe JA, Jiang BH, Iyer NV, Agani F, Leung SW, Koos RD, et al. Activation of vascular endothelial growth factor gene transcription by hypoxia-inducible factor 1. Mol Cell Biol 1996;16:4604–13.
6. Nagy JA, Chang S, Dvorak AM, Dvorak HF. Why are tumour blood vessels abnormal and why is it important to know? Br J Cancer 2009;100:865–9.
7. Hashizume H, Baluk P, Morikawa S, McLean JW, Thurston G, Roberge S, et al. Openings between defective endothelial cells explain tumor vessel leakiness. Am J Pathol 2000;156:1363–80.
8. Stylianopoulos T, Jain RK. Combining two strategies to improve perfusion and drug delivery in solid tumors. Proc Natl Acad Sci U S A 2013;110:18632–7.
9. Horsman M, Wouters BG, Joiner M, Overgaard J. The oxygen effect and fractionated radiotherapy. In: Basic clinical radiobiology. London: Hodder Arnold, 2009. p.207–15.
10. Overgaard J. Hypoxic radiosensitization: Adored and ignored. J Clin Oncol 2007;25:4066–74.
11. De Bock K, Cauwenberghs S, Carmeliet P. Vessel abnormalization: another hallmark of cancer? Molecular mechanisms and therapeutic implications. Curr Opin Genet Dev 2011;21:73–9.
12. Horsman MR, van der Kogel A. Therapeutic approaches to tumor hypoxia. In: Basic clinical radiobiology. London: Hodder Arnold, 2009. p.242–4.
13. Saharinen P, Eklund L, Alitalo K. Therapeutic targeting of the angiopoietin-TIE pathway. Nat Rev Drug Discov 2017;16:635–61.
14. Jeansson M, Gawlik A, Anderson G, Li C, Kerjaschki D, Henkelman M, et al. Angiopoietin-1 is essential in mouse vasculature during development and in response to injury. J Clin Invest 2011;121:2278–89.
15. Kwak HJ, Lee SJ, Lee Y, Ryu CH, Koh KN, Choi HY, et al. Angiopoietin-1 inhibits irradiation- and mannitol-induced apoptosis in endothelial cells. Circulation 2000;101:2317–24.
16. Daly C, Pasnikowski E, Burova E, Wong V, Aldrich TH, Griffiths J, et al. Angiopoietin-2 functions as an autocrine protective factor in stressed endothelial cells. Proc Natl Acad Sci U S A 2006;103:15491–6.
17. Daly C, Eichten A, Castanaro C, Pasnikowski E, Adler A, Lalani AS, et al. Angiopoietin-2 functions as a Tie2 agonist in tumor models, where it limits the effects of VEGF inhibition. Cancer Res 2013;73:108–18.
18. Simon M, Tournaire R, Pouyssegur J. The angiopoietin-2 gene of endothelial cells is up-regulated in hypoxia by a HIF binding site located in its first intron and by the central factors GATA-2 and ets-1. J Cell Physiol 2008;217:809–18.
19. Helfrich I, Edler L, Sucker A, Thomas M, Christian S, Schadendorf D, et al. Angiopoietin-2 levels are associated with disease progression in metastatic malignant melanoma. Clin Cancer Res 2009;15:1384–92.
20. Takanami I.Overexpression of ang-2 mRNA in non-small cell lung cancer: association with angiogenesis and poor prognosis. Oncol Rep 2004;12:849–53.
21. Eggert A, Ikegaki N, Kwiatkowski J, Zhao H, Brodeur GM, Himelstein BP. High-level expression of angiogenic factors is associated with advanced tumor stage in human neuroblastomas. Clin Cancer Res 2000;6:1900–8.
22. Lee WH, Cho HJ, Sonntag WE, Lee YW. Radiation attenuates physiological angiogenesis by differential expression of VEGF, ang-1, tie-2 and ang-2 in rat brain. Radiat Res 2011;176:753–60.

23. Peterson TE, Kirkpatrick ND, Huang Y, Farrar CT, Marijt KA, Kloepper J, et al. Dual inhibition of ang-2 and VEGF receptors normalizes tumor vasculature and prolongs survival in glioblastoma by altering macrophages. Proc Natl Acad Sci U S A 2016;113:4470–5.
24. D'Amico G, Korhonen EA, Anisimov A, Zarkada G, Holopainen T, Hägerling R, et al. Tie1 deletion inhibits tumor growth and improves angiopoietin antagonist therapy. J Clin Invest 2014;124:824–34.
25. Papadopoulos K, Kelley R, Tolcher A, Razak A, Van Loon K, Patnaik A, et al. A phase I first-in-human study of nesvacumab (REGN910), a fully human anti-angiopoietin-2(Ang2) monoclonal antibody, in patients with advanced solid tumors. Clin Cancer Res 2016;22:1348–55.
26. Hyman DM, Rizvi N, Natale R, Armstrong DK, Birrer M, Recht L, et al. Phase I Study of MEDI3617, a selective angiopoietin-2 inhibitor alone and combined with carboplatin/paclitaxel, paclitaxel, or bevacizumab for advanced solid tumors. Clin Cancer Res 2018;24:2749–2757.
27. Holopainen T, Saharinen P, D'Amico G, Lampinen A, Eklund L, Sormunen R, et al. Effects of angiopoietin-2-blocking antibody on endothelial cell-cell junctions and lung metastasis. J Natl Cancer Inst 2012;104:461–75.
28. Rigamonti N, Kadioglu E, Keklikoglou I, Rmili CW, Leow CC, de Palma M. Role of angiopoietin-2 in adaptive tumor resistance to VEGF signaling blockade. Cell Rep 2014;8:696–706.
29. Bracci L, Schiavoni G, Sistigu A, Belardelli F. Immune-based mechanisms of cytotoxic chemotherapy: Implications for the design of novel and rationale-based combined treatments against cancer. Cell Death Differ 2014;21:15–25.
30. Schaue D.A century of radiation therapy and adaptive immunity. Front Immunol 2017;8:431.
31. Mazzieri R, Pucci F, Moi D, Zonari E, Ranghetti A, Berti A, et al. Targeting the ANG2/TIE2 axis inhibits tumor growth and metastasis by impairing angiogenesis and disabling rebounds of proangiogenic myeloid cells. Cancer cell 2011;19:512–26.
32. Baumann M, Grégoire V. Molecular-targeted agents for enhancing tumour response. In: Basic clinical radiobiology. London: Hodder Arnold, 2009. p.291.
33. Grégoire V, Baumann M. Combined radiotherapy and chemotherapy. In: Basic clinical radiobiology. London: Hodder Arnold, 2009. p.246–54.
34. Dewan MZ, Galloway AE, Kawashima N, Dewyngaert JK, Babb JS, Formenti SC, et al. Fractionated but not single-dose radiotherapy induces an immune-mediated abscopal effect when combined with anti-CTLA-4 antibody. Clin Cancer Res 2009;15:5379–88.
35. Dovedi SJ, Cheadle EJ, Popple AL, Poon E, Morrow M, Stewart R, et al. Fractionated radiation therapy stimulates antitumor immunity mediated by both resident and infiltrating polyclonal T-cell populations when combined with PD-1 blockade. Clin Cancer Res 2017;23:5514–26.
36. Wachsberger P, Burd R, Dicker AP. Tumor response to ionizing radiation combined with antiangiogenesis or vascular targeting agents: Exploring mechanisms of interaction. Clin Cancer Res 2003;9:1957–71.
37. Williams KJ, Telfer BA, Shannon AM, Babur M, Stratford IJ, Wedge SR. Inhibition of vascular endothelial growth factor signalling using cediranib (RECENTINTM; AZD2171) enhances radiation response and causes substantial physiological changes in lung tumour xenografts. Br J Radiol 2008;81:S21–7.
38. Nieder C, Wiedenmann N, Andratschke N, Molls M. Current status of angiogenesis inhibitors combined with radiation therapy. Cancer Treat Rev 2006;32:348–64.
39. Goel S, Gupta N, Walcott BP, Snuderl M, Kesler CT, Kirkpatrick ND, et al. Effects of vascular-endothelial protein tyrosine phosphatase inhibition on breast cancer vasculature and metastatic progression. J Natl Cancer Inst 2013;105:1188–201.
40. Jackson RA, Chen ES.Synthetic lethal approaches for assessing combinatorial efficacy of chemotherapeutic drugs. Pharmacol Ther 2016;162:69–85.
41. Wu X, Giobbie-Hurder A, Liao X, Connelly C, Connolly E, Li J, et al. Angiopoietin-2 as a biomarker and target for immune checkpoint therapy. Cancer Immunol Res. 2017;5:17–28.
42. Schmittnaegel M, Rigamonti N, Kadioglu E, Cassara A, Wyser Rmili C, Kiialainen A, et al. Dual angiopoietin-2 and VEGFA inhibition elicits antitumor immunity that is enhanced by PD-1 checkpoint blockade. Sci Transl Med 2017;9:eaak9670
43. Singhal M, Augustin HG. Beyond angiogenesis: exploiting angiocrine factors to restrict tumor progression and metastasis. Cancer Res. 2020:80:659–62